MÜHENDİSLİK FAKÜLTESİ

Uluslararası Mühendislik Araştırma ve Geliştirme Dergisi

International Journal of Engineering Research and Development

Cilt/Volume:10 Sayı/Issue:1 Ocak/January 2018 https://doi.org/10.29137/umagd.349654

Araştırma Makalesi / Research Article

Numerical Solution of Thermal Residual Stress Analysis with Finite Difference Method of Functionally Graded Circular Plates

M. Didem DEMİRBAŞ*[1], M. Kemal APALAK[1]

[1]Erciyes University, Faculty of Engineering, Department of Mechanical Engineering 38039 Talas, Kayseri, TURKEY

Başvuru/Received: 06/10/2017 **Kabul/Accepted**: 15/12/2017 **Son Versiyon/Final Version**: 29/01/2018

Abstract

In this study, thermal residual stress analysis of functionally graded circular plates (FGCP) carried out. Finite difference equations are used in solving Navier's equations of elasticity and Fourier's heat conduction equation. The grading along the plate was made along the surface of plate and it was assumed that the material properties changed according to the Mori-Tanaka approach. Grading along the plate was made in both radial and tangential directions. In this study, the effect of the coordinate derivatives of material properties was taken into consideration in both Fourier's heat conduction equation and Navier's equations of elasticity, unlike the other studies. As a result, when the materials compositions of FGCP were changed from ceramic-rich to metal-rich compositions, the stress levels were not affected considerably. The strain levels increased significantly when the metal compound in the material composition of FGCP was increased. FGCP are emphasized that the change of material properties due to two-dimensional significantly affect distributions of thermal strain and stress. In this study, it was emphasized that changing the radial and tangential direction of the compositional gradient exponents of FGCP subjected to heat flux along the outer edge significantly influences the strain and stress distributions.

Key Words

"Functionally graded circular plates, Finite difference methods, Thermal residual stress"

*** mddemirbas@erciyes.edu.tr***

1. INTRODUCTION

The functionally gradient materials (FGMs) are one kind of the high technology materials that have been researched to decrease thermal stresses and to eliminate discontinuous stress concentrations (Noda, 1999). FGMs overcome the disadvantage of the conventional composites plates that have been used as thermal barriers in the space planes, ultra-super-hypersonic airplanes for the super-sonic transport, nuclear fusion reactors, and similar structures (Choules & Kokini, 1996). In many studies have focused thermo-elastic or plastic stress analyses on the one- or two-dimensional functionally graded plates, and these structures are assumed as a functionally graded composition variation through the thickness.

Recent studies have focused thermo-elastic or plastic stress analyses on the one- or two-dimensional functionally graded plates, and these structures were assumed functionally graded composition variations through the thickness.

Apalak & Demirbas (2013) analyzed the thermo-elastic response of functionally graded plates and adhesively bonded functionally graded rectangular and circular hollow plates independent subjected to an in-plane different heat flux. They expressed that type of in-plane heat flux affected heat transfer period and temperature levels, the residual thermal stresses were strongly dependent on the in-plane material composition gradient and could be decreased by altering in-plane material composition. Wang et al., (2004) researched the thermal shock resistance of FGMs. Their studies yielded explicit expressions for 1-D transient thermal conduction for a plate, shell and sphere. Thermal shock analysis of FGM plate exposed to different circumferential temperatures was performed with a finite element/finite different method.

Moosaie (2016) performed a nonlinear thermo-elastic analysis of a functionally graded thick-walled cylinder. He presented analytic solution of the non-linear heat conduction equation for a functionally graded thick-walled cylinder and obtained a temperature field using a perturbation technique. The exact solutions of elasticity equations were developed for incompressible elastic material, and stress results were obtained. Mahdavi et al., (2016) studied the thermo-mechanical behavior of functionally graded rotating discs. Their study was based on the variable material property theory and their theoretical results were compared with solutions obtained by the finite element method (FEM). The thermo mechanical properties were assumed to be constant and elastic-plastic problems were solved using the form of the elastic response. They emphasized that the method can be used to solve both elastic and elasto-plastic problems and that temperature-dependent material properties should be taken into account in the solution of the problem. Najibi and Talebitooti (2017) performed the transient thermo-elastic analysis of a thick hollow finite length cylinder made of two-dimensional functionally graded materials. Transient heat conduction and thermos-elastic equations were solved for the cylinder subjected to thermal loading using the FEM. They emphasized that the variation of the material distribution in the axial direction changes the temperature and stress distributions significantly. Burlayenko et al., (2017) developed a model for solving functionally graduated two-dimensional plates by plane-shape transformation using the FEM. When comparing the results with the literature, they emphasized that the developed finite element model gave very good results regarding temperature fields and thermally induced stress distributions. Swaminathan and Sangeetha (2017) conducted a comprehensive review of the various developments, applications, various mathematical material distributions, temperature profiling, modeling techniques and solution methods accepted for thermal analysis of functionally graded plates. Ghannad and Parhizkar Yaghoobi (2017) presented a thermal elastic analysis of the axially symmetric FGM cylinder subjected to pressure on the inner surface and heat flux on the outer surface. As a result, she stressed that the shear stress was effective on the cylinder edges and that the temperature and displacement fields changed depending on the length of the cylinder. Nowadays, fuel cell technology applies successfully FGMs to solid oxide fuel cells in order to reduce thermal expansion coefficient mismatch between electrolyte and anode examined inclusively five categories of fuel cells, and related studies (Iwasawa et al.,1997- Wang, et al., 2011) Fuel cells are popular examples that conductive and convective heat transfers, and mass transfer, multiple fluids flows moreover electrochemical reactions are experienced (Kakac, 2007, Ruys, 2001, Noda, 1997). Consequently, a tubular or planar design of a solid oxide fuel cell can experience in-plane or through-thickness heat transfer due to heat fluxes. Thus, an in-plane one- or two-dimensional functionally graded material distribution requires a theoretical investigation for the practical applications.

Many studies in the literature focus on functionally graded circular or rectangular plates and structures in one- or two- dimensions (through-thickness or radial direction) under thermal load. For numerical solutions, FEM was generally used as a solution method and functional grading was performed along the thickness. In this study, the thermal stress behavior of two-dimensional circular plates was investigated. The grading on the plate was made along the plane, not along the thickness. Two-dimensional thermo-elastic problem for plane strain and plane strain in numerical solution is solved by using FDM. In the equations used for the thermo-elastic solution, the effect of the directional dependence of the material properties is considered.

2. MATERIALS AND METHODS

In this problem, the FGCP have a material composition of two constituents, ceramic and metal, and the material composition is two-directional in the plate plane. In addition, the effect of the directional dependence of the material properties is taken into consideration in both Heat Transfer and Navier's Equations, unlike the other studies.

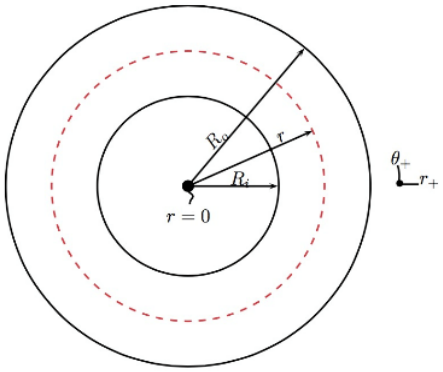

Figure 1: Functionally graded circular plate

2.1. Material Properties

In this study, it is assumed that homogeneous, isotropic grading is designed in the radial and tangential directions between the ceramic and metal phases of the FGCP. The volume fraction of the ceramic (c) phase in each position in the radial and tangential direction, respectively

$$V_c^r(\bar{r}) = \left(\frac{\bar{r}}{l_R}\right)^n \tag{1}$$

$$V_c^\theta(\theta) = (|\sin(p\theta)|)^m \tag{2}$$

n and m compositional gradient exponents along the radial and tangential directions, respectively, $\bar{r}=r-R_i$ is the radial distance from the inner edge of the circular plate, and $l_R=R_o-R_i$ is the circular plate length. R_i and R_o are the inner and outer radius of the circular plate, respectively. p=0.5 is a period of periodic functions. The ceramic volume fraction of the plate abides by the power law as (Nemat-Alla, 2003)

$$V_c(\bar{r},\theta) = V_c^r(\bar{r})V_c^\theta(\theta) \tag{3}$$

for the metal volume fraction of the plate,

$$V_m(\bar{r},\theta) = 1 - V_c(\bar{r},\theta) \tag{4}$$

where r and θ are considered as distance along in-plane radial and tangential directions, respectively.

The thermal, physical and mechanical properties of the constituents of Ni and Al_2O_3 composite material are explained in Table 1.

Table 1: The thermal, physical and mechanical properties of metal (Ni) and ceramic (Al2O3) used (Materials Information Resource MatWeb, 2016)

Property	Unit	Ni	Al_2O_3
Density, ρ	kg/m^3	8880	3960
Thermal conductivity, k	W/m-K	60.5×10^{-3}	46×10^{-3}
Specific heat capacity, c_p	W-h/kg-K	0.11	0.21
Shear modulus, G	GPa	76	150
Bulk modulus, K	GPa	180	172
Coefficient of thermal expansion, α	1/C	6.6×10^{-6}	8.1×10^{-6}

The simple estimation method is the linear rule of the mixtures in which a material properties P at any point r in the graded region are determined.

$$P(r) = V_c(r)P_c(r) + V_m(r)P_m(r) \tag{5}$$

Tomota et al., (1976) offered a mixtures rule for the elasticity modulus as Wakashima & Tsukamoto (1991) makes statement necessitate that the overall thermal expansion coefficient (α) for a diphase material is connected the averaged bulk modulus (K) using the Levin (1967) relation. Other material properties have been accepted to change according to the Mori &Tanaka approach (1973).

2.2. Heat Transfer

In the transient two-dimensional Fourier's heat conduction equation heat conductivity coefficient (λ), density (ρ), specific heat capacity (cp) varies in both radial and tangential directions,

$$\vec{\nabla}\left(\lambda\vec{\nabla}T\right) = \rho c_p \frac{\partial T}{\partial t} \tag{6}$$

$$\frac{\partial\lambda}{\partial r}\frac{\partial T}{\partial r} + \frac{1}{r^2}\frac{\partial\lambda}{\partial\theta}\frac{\partial T}{\partial\theta} + \frac{\lambda}{r}\frac{\partial T}{\partial r} + \lambda\frac{\partial^2 T}{\partial r^2} + \frac{\lambda}{r^2}\frac{\partial^2 T}{\partial\theta^2} = \rho c_p \frac{\partial T}{\partial t} \tag{7}$$

T (r, θ, t) at the nodal point (i, j) with the coordinate (r,θ) or with respect to time t and the space variables (r,θ). Herewith, the heat transfer equation can be written in terms of difference equations as (for the internal grid points along i= [2: nr-1] and j= [2: nw-1]),

$$T_{i,j}^{k+1} = T_{i,j}^{k} + \frac{\Delta t}{(\rho c_p)_{i,j}\Delta r}\left(\lambda_{i+1,j} - \lambda_{i,j}\right)\frac{1}{\Delta r}\left(T_{i+1,j}^{k} - T_{i,j}^{k}\right) + \frac{\Delta t}{(\rho c_p)_{i,j}(r_{i,j})^2(\Delta\theta)^2}\left(\lambda_{i,j+1} - \lambda_{i,j}\right)\left(T_{i,j+1}^{k} - T_{i,j}^{k}\right) + \frac{\lambda_{i,j}\Delta t}{(\rho c_p)_{i,j} r_{i,j}\Delta r}\left(T_{i+1,j}^{k} - T_{i,j}^{k}\right) + \frac{\lambda_{i,j}\Delta t}{(\rho c_p)_{i,j}(\Delta r)^2}\left(T_{i+1,j}^{k} - 2T_{i,j}^{k} + T_{i-1,j}^{k}\right) + \frac{\lambda_{i,j}\Delta t}{(\rho c_p)_{i,j}(r_{i,j})^2(\Delta\theta)^2}\left(T_{i,j+1}^{k} - 2T_{i,j}^{k} + T_{i,j-1}^{k}\right) \tag{8}$$

for all grid points at i=1 and j= [1: nw],

$$T_{i,j}^{k+1} = T_{i,j}^{k} + \frac{\Delta t}{(\rho c_p)_{i,j}\Delta r}\left(\lambda_{i+1,j} - \lambda_{i,j}\right)\frac{1}{\Delta r}\left(T_{i+1,j}^{k} - T_{i,j}^{k}\right) + \frac{\Delta t}{(\rho c_p)_{i,j}(r_{i,j})^2(\Delta\theta)^2}\left(\lambda_{i,j+1} - \lambda_{i,j}\right)\left(T_{i,j+1}^{k} - T_{i,j}^{k}\right) + \frac{\lambda_{i,j}\Delta t}{(\rho c_p)_{i,j} r_{i,j}\Delta r}\left(T_{i+1,j}^{k} - T_{i,j}^{k}\right) + \frac{\lambda_{i,j}\Delta t}{(\rho c_p)_{i,j}(\Delta r)^2}\left(-T_{i+3,j}^{k} + 4T_{i+2,j}^{k} - 5T_{i+1,j}^{k} + 2T_{i,j}^{k}\right) + \frac{\lambda_{i,j}\Delta t}{(\rho c_p)_{i,j}(r_{i,j})^2(\Delta\theta)^2}\left(T_{i,j+1}^{k} - 2T_{i,j}^{k} + T_{i,j-1}^{k}\right) \tag{9}$$

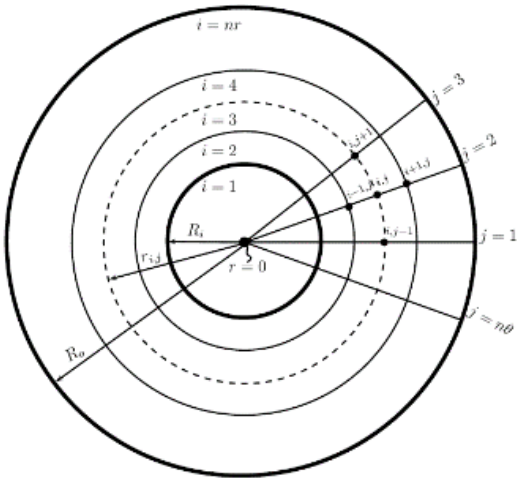

Figure 2: Finite difference grit of plate

for all grid points at i=nr and j= [1: nw],

$$T_{i,j}^{k+1} = T_{i,j}^{k} + \frac{\Delta t}{(\rho c_p)_{i,j}\Delta r}\left(\lambda_{i,j} - \lambda_{i-1,j}\right)\frac{1}{\Delta r}\left(T_{i,j}^{k} - T_{i-1,j}^{k}\right) + \frac{\Delta t}{(\rho c_p)_{i,j}(r_{i,j})^2(\Delta\theta)^2}\left(\lambda_{i,j+1} - \lambda_{i,j}\right)\left(T_{i,j+1}^{k} - T_{i,j}^{k}\right) + \frac{\lambda_{i,j}\Delta t}{(\rho c_p)_{i,j} r_{i,j}\Delta r}\left(T_{i,j}^{k} - T_{i-1,j}^{k}\right) + \frac{\lambda_{i,j}\Delta t}{(\rho c_p)_{i,j}(\Delta r)^2}\left(-T_{i-3,j}^{k} + 4T_{i-2,j}^{k} - 5T_{i-1,j}^{k} + 2T_{i,j}^{k}\right) + \frac{\lambda_{i,j}\Delta t}{(\rho c_p)_{i,j}(r_{i,j})^2(\Delta\theta)^2}\left(T_{i,j+1}^{k} - 2T_{i,j}^{k} + T_{i,j-1}^{k}\right) \tag{10}$$

this equations can be arranged on thermal equilibrium of that cell as follows: for all grid points at

i= [2: nr-1], j=1 to $j-1 \rightarrow nw$ (11)

i= [2: nr-1], j=nw to $j+1 \rightarrow 1$ (12)

are written.

2.2.1. Initial and Boundary Conditions

The initial temperature is given as $T(r,\theta)$=298 K at t=0, and thermal boundary conditions are given as:

$$q_i = q(R_i, \theta, t) \tag{13}$$

$$q_o = q(R_o, \theta, t) = 200 KW/m^2 \tag{14}$$

Where q_i and q_o are inner and outer heat fluxes along the radial direction r, respectively. The boundary condition, the inner edge is subjected to adiabatic conditions while the outer boundary is subjected to heat flux. The initial temperature is taken as 298 K for the whole circular plate and the analysis is completed when the temperature reached 900 K at any point along the outer edge of the plate. The inner and outer radius of plate is 100 mm and 200 mm, respectively. FGCPs have a radial length l=100 mm and thickness t=1mm. As the 1 mm plate thickness is much smaller than other dimensions, the stress and strain in the thickness direction were neglected and a 2-D analyses is conducted.

If the first boundary condition is adapted to the two-dimensional heat transfer equation, (along the outer edge of the circular plate ($r_{nr,j}$= R_o) with (i=1, j= [1: nw]))

$$\frac{(\rho c_p)_{i,j}}{\lambda_{i,j}\Delta t}\left(T_{i,j}^{k+1} - T_{i,j}^{k}\right) = \frac{2q_e}{\lambda_{i,j}\Delta r} + \frac{2}{(\Delta r)^2}\left(T_{i-1,j}^{k} - T_{i,j}^{k}\right) + \frac{1}{(\Delta\theta)^2}\left(T_{i,j+1}^{k} - T_{i,j}^{k}\right) + + \frac{1}{(\Delta\theta)^2}\left(T_{i,j-1}^{k} - T_{i,j}^{k}\right) \tag{15}$$

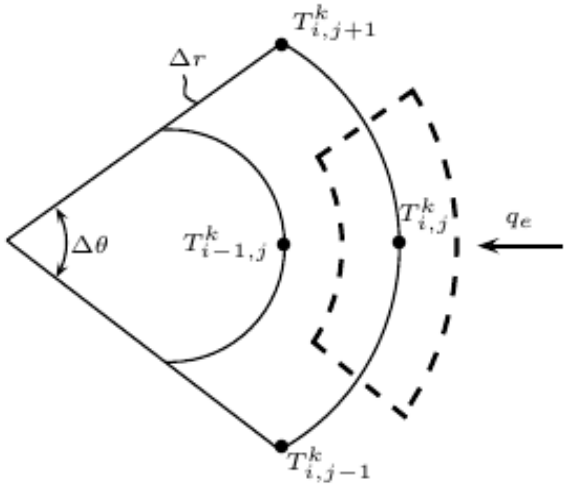

Figure 3: Outer edge of plate

If the second boundary condition is adapted to the two-dimensional heat transfer equation, (along the inner edge of the circular plate ($r_{nr,j}$= R_i) with (i=1, j= [1: nw]))

$$\frac{(\rho c_p)_{i,j}}{\lambda_{i,j}\Delta t}\left(T_{i,j}^{k+1} - T_{i,j}^{k}\right) = \frac{2q_f}{\lambda_{i,j}\Delta r} + \frac{2}{(\Delta r)^2}\left(T_{i+1,j}^{k} - T_{i,j}^{k}\right) + \frac{1}{(\Delta\theta)^2}\left(T_{i,j+1}^{k} - T_{i,j}^{k}\right) + + \frac{1}{(\Delta\theta)^2}\left(T_{i,j-1}^{k} - T_{i,j}^{k}\right) \tag{16}$$

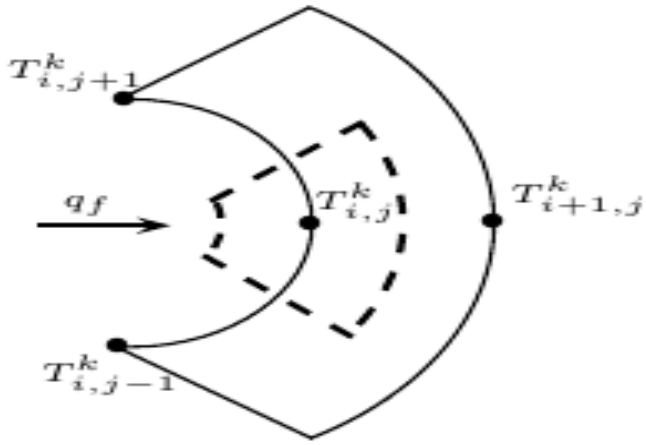

Figure 4: Inner edge of plate

2.3. Navier's Equations of Elasticity

Two-dimensional Navier's equations of elasticity in the radial and tangential directions are written as ($T=T(r,\theta,t)-T_o$ is the temperature difference)

$$2\frac{\partial u}{\partial r}\frac{\partial \mu}{\partial r}+\left(\frac{\partial u}{\partial r}+\frac{1}{r}\frac{\partial v}{\partial \theta}+\frac{u}{r}\right)\frac{\partial \lambda}{\partial r}+\frac{\lambda}{r}\frac{\partial u}{\partial r}-\frac{\lambda}{r^2}\frac{\partial v}{\partial \theta}+\frac{\lambda}{r}\frac{\partial^2 v}{\partial r\partial\theta}+(2\mu+\lambda)\frac{\partial^2 u}{\partial r^2}-\frac{\lambda}{r^2}u\left(\frac{1}{r^2}\frac{\partial u}{\partial \theta}+\frac{1}{r}\frac{\partial v}{\partial r}-\frac{v}{r^2}\right)\frac{\partial \mu}{\partial \theta}-\frac{\mu}{r^2}\frac{\partial v}{\partial \theta}+\frac{\mu}{r^2}\frac{\partial^2 u}{\partial \theta^2}+\frac{\mu}{r}\frac{\partial^2 v}{\partial r\partial\theta}+\frac{2\mu}{r}\frac{\partial u}{\partial r}-\frac{2\mu}{r^2}\frac{\partial v}{\partial \theta}+\frac{2\mu}{r^2}u-3\alpha T\frac{\partial \lambda}{\partial r}-2\alpha T\frac{\partial \mu}{\partial r}-(3\lambda+2\mu)T\frac{\partial \alpha}{\partial r}-(3\lambda+2\mu)\alpha\frac{\partial T}{\partial r}=0 \quad (17)$$

$$2\frac{\partial u}{\partial r}\frac{\partial \mu}{\partial r}+\left(\frac{\partial u}{\partial r}+\frac{1}{r}\frac{\partial v}{\partial \theta}+\frac{u}{r}\right)\frac{\partial \lambda}{\partial r}+\left(\frac{1}{r^2}\frac{\partial u}{\partial \theta}+\frac{1}{r}\frac{\partial v}{\partial r}-\frac{v}{r^2}\right)\frac{\partial \mu}{\partial \theta}+\frac{(\lambda+2\mu)}{r}\frac{\partial u}{\partial r}-\frac{(\lambda+3\mu)}{r^2}\frac{\partial v}{\partial \theta}+\frac{(\lambda+\mu)}{r}\frac{\partial^2 v}{\partial r\partial\theta}+(\lambda+2\mu)\frac{\partial^2 u}{\partial r^2}+\frac{\mu}{r^2}\frac{\partial^2 u}{\partial \theta^2}-\frac{(\lambda+2\mu)}{r^2}u-3\alpha T\frac{\partial \lambda}{\partial r}-2\alpha T\frac{\partial \mu}{\partial r}-(3\lambda+2\mu)T\frac{\partial \alpha}{\partial r}-(3\lambda+2\mu) \quad (18)$$

In equations (17) and (18), the thermal stress equations are written for the entire plate by choosing the appropriate ones from the equations (19)-(30) for the finite difference equations with the first and second order derivatives (in the inner region and edges of the plate).

$$\left(\frac{\partial \varpi}{\partial r}\right)_{i,j}=\frac{\varpi_{i+1,j}-\varpi_{i,j}}{\Delta r} \quad (19)$$

$$\left(\frac{\partial \varpi}{\partial r}\right)_{i,j}=\frac{\varpi_{i,j}-\varpi_{i-1,j}}{\Delta r} \quad (20)$$

$$\left(\frac{\partial \varpi}{\partial \theta}\right)_{i,j}=\frac{\varpi_{i,j+1}-\varpi_{i,j}}{\Delta \theta} \quad (21)$$

$$\left(\frac{\partial \varpi}{\partial \theta}\right)_{i,j}=\frac{\varpi_{i,j}-\varpi_{i,j-1}}{\Delta \theta} \quad (22)$$

$$\left(\frac{\partial^2 \varpi}{\partial r^2}\right)_{i,j}=\frac{\varpi_{i+1,j}-2\varpi_{i,j}+\varpi_{i-1,j}}{(\Delta r)^2} \quad (23)$$

$$\left(\frac{\partial^2 \varpi}{\partial \theta^2}\right)_{i,j}=\frac{\varpi_{ij+1}-2\varpi_{i,j}+\varpi_{i,j-1}}{(\Delta \theta)^2} \quad (24)$$

$$\left(\frac{\partial^2 \varpi}{\partial r^2}\right)_{i,j}=\frac{-\varpi_{i+3,j}+4\varpi_{i+2,j}-5\varpi_{i+1,j}+2\varpi_{i,j}}{(\Delta r)^2} \quad (25)$$

$$\left(\frac{\partial^2 \varpi}{\partial \theta^2}\right)_{i,j}=\frac{-\varpi_{i,j+3}+4\varpi_{i,j+2}-5\varpi_{i,j+1}+2\varpi_{i,j}}{(\Delta \theta)^2} \quad (26)$$

$$\left(\frac{\partial^2 \varpi}{\partial r^2}\right)_{i,j} = \frac{-\varpi_{i-3,j}+4\varpi_{i-2,j}-5\varpi_{i-1,j}+2\varpi_{i,j}}{(\Delta r)^2} \quad (27)$$

$$\left(\frac{\partial^2 \varpi}{\partial \theta^2}\right)_{i,j} = \frac{-\varpi_{i,j-3}+4\varpi_{i,j-2}-5\varpi_{i,j-1}+2\varpi_{i,j}}{(\Delta \theta)^2} \quad (28)$$

$$\left(\frac{\partial^2 \varpi}{\partial r \partial \theta}\right)_{i,j} = \frac{\varpi_{i,j+1}-\varpi_{i,j}-\varpi_{i-1,j+1}+\varpi_{i-1,j}}{\Delta r \Delta \theta} \quad (29)$$

$$\left(\frac{\partial^2 \varpi}{\partial r \partial \theta}\right)_{i,j} = \frac{\varpi_{i,j}-\varpi_{i,j-1}-\varpi_{i-1,j}+\varpi_{i-1,j-1}}{\Delta r \Delta \theta} \quad (30)$$

If the figures contain dark or colored areas, the figures should be checked on high quality, colorless laser printers to ensure that they can be printed properly. The figures used in the text of the paper are gray, only the images can be colored.

2.3.1. Initial and Boundary Conditions

The circular plate is fixed along all its edges (u (r, θ) =0 and v (r, θ) =0).

The material is completely ceramic (Al_2O_3) at the edge outer of the plate where r =R_o, and the material is completely metal (Ni) the inner edge of the plate (r = R_i). A one-dimensional grading is performed along radial direction with three different compositional gradient exponents of n = 0.1 (ceramic rich compound), 0.5, and 1.0 (linear change is from ceramic rich compound to metal rich compound).

FDM requires that the plate be divided into a grid of nr = 80 x nq = 240 divisions along the coordinates r and θ, respectively. The temperature matrix obtained from the heat transfer solution is considered as the temperature difference in the Navier equations. The appropriate finite difference equations are selected for the internal points, edges and corners of the plate. The implicit difference equations of the stress analysis are coded, solved and post-processed graphically in MATLAB (Mathematical software, 2009).

3.RESULTS

As can be seen in Figure 6, as the compositional gradient exponent ('n') in the radial direction increases, the equivalent strain levels increase and the maximum strain areas expands. The reason for this increase is the increase in the metal volume ratio, which is less resistant to heat in the material composition. As the compositional gradient exponent ('m') in the angular direction increases, the equivalent strain levels do not change but the maximum strain areas around θ=0º are narrowed.

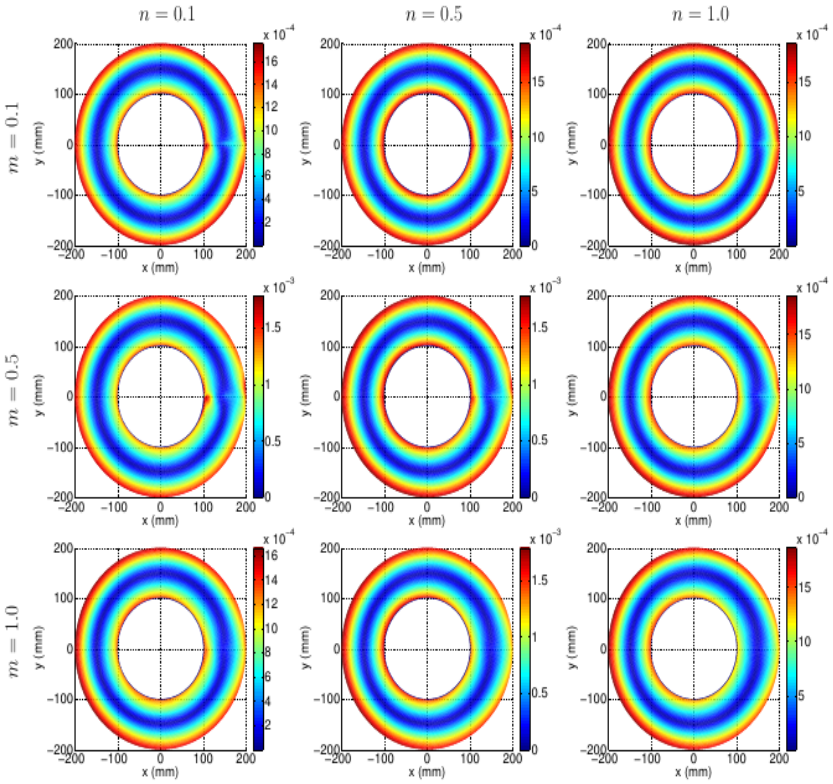

Figure 6: Distribution of the in-plane equivalent strain along the plate for different compositional gradients

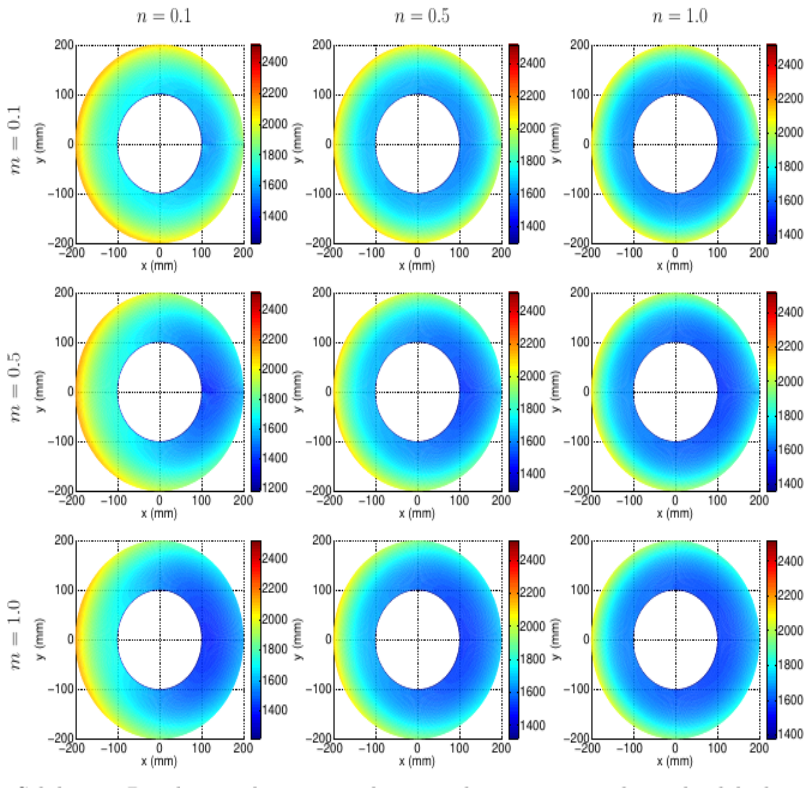

Figure 7: Distribution of the in-plane equivalent stress along the plate for different compositional gradients

As can be seen in Figure 8, the equilibrium stress levels do not change significantly as the compositional gradient exponent ('n') in the radial direction increases. However, the equivalent stress bands at maximum and medium levels are narrowing outward from the inside of the plate, around θ=180º. As the compositional gradient exponent value ('m') in the angular direction increases, the equivalent stress levels do not change but at θ=0º, the areas affected by the maximum and middle stress bands are symmetrically narrowed at the top and bottom of the plate.

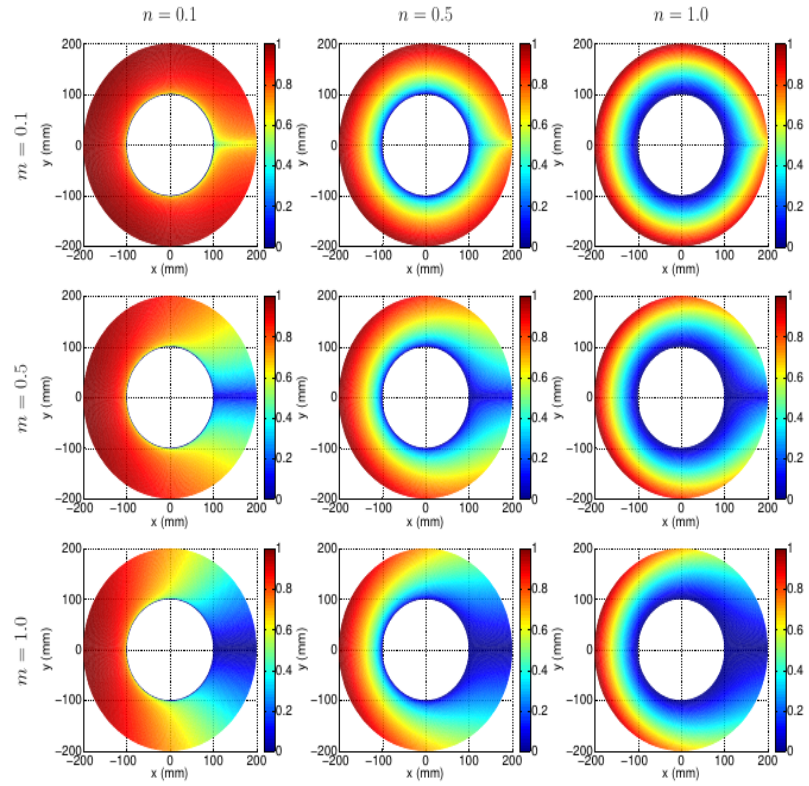

Figure 8: Distribution of the in-plane ceramic volume fractions along the plate for different compositional gradients

As shown in Figure 7, the equivalent stress distribution along the plate is dependent on the compositional gradient exponent. Therefore, the effectiveness of the compositional gradient exponent is important when the appropriate working conditions of the plate are determined.

4. CONCLUSIONS

In the theoretical thermal stress analysis, it is important to take into account the effect of coordinate derivatives of material properties and to grade the FGCP in two directional for optimum design.

REFERENCES

Noda, N. (1999). Thermal stress intensity factor for functionally gradient plate with an edge crack. Journal of Thermal Stresses, 22(4-5), 477-512.

Choules, B.D., & Kokini, K. (1996). Architecture of functionally graded ceramic coatings against surface thermal fracture. Journal of Engineering Materials and Technology, 118(4), 522-528.

Apalak, M.K., & Demirbas, M.D. (2013). Thermal residual stresses in adhesively bonded in-plane functionally graded clamped circular hollow plate. Journal of Adhesion Science and Technology, 27(14),1590-1623.

Wang, B.L., Mai, Y.W., & Zhang, X.H. (2004). Thermal shock resistance of functionally graded materials. Acta Materialia, 52(17), 4961-4972.

Moosaie, A. (2016). A nonlinear analysis of thermal stresses in an incompressible functionally graded hollow cylinder with temperature-dependent material properties. European Journal of Mechanics A/Solids, 55, 212-220.

Mahdavia, E., Ghasemib, A., & Akbari Alashtic, R. (2016). Elastic-plastic analysis of functionally graded rotating disks with variable thickness and temperature-dependent material properties under mechanical loading and unloading. Aerospace Science and Technology, 59, 57-68.

Najibi, A., & Talebitooti, R., (2017). Nonlinear transient thermo-elastic analysis of a 2D-FGM thick hollow finite length cylinder. Composites Part B: Engineering, 111, 211-227.

Burlayenko, V.N., Altenbach, H., Sadowski, T., Dimitrova, S.D., & Bhaskar, A. (2017). Modelling functionally graded materials in heat transfer and thermal stress analysis by means of graded finite elements. Applied Mathematical Modelling, 45, 422-438.

Swaminathan, K., Sangeetha, D.M. (2017). Thermal analysis of FGM plates - A critical review of various modeling techniques and solution methods. Composite Structures, 160, 43-60.

Ghannad, M., Parhizkar Yaghoobi, M. (2017). 2D thermo elastic behavior of a FG cylinder under thermomechanical loads using a first order temperature theory. International Journal of Pressure Vessels and Piping, 149, 75-92

Iwasawa C., Nagata, M., Seino, Y., & Ono, M. (1997). A study on anode materials and structures for SOFC. Proceedings of the Fifth International Symposium on Solid Oxide Fuel Cells (SOFC-V), 97(40), 626-634.

Wang, Y., Chen, K.S., Mishler, J., Cho, S.C., & Adroher, X.C. (2011). A review of polymer electrolyte membrane fuel cells: Technology, applications, and needs on fundamental research. Applied Energy, 88(4), 981-1007.

Kakac, S., Pramuanjaroenkij, A., & Zhou, X.Y. (2007). A review of numerical modeling of solid oxide fuel cell. International Journal of Hydrogen Energy, 32(7), 761-786.

Ruys, A., Popov, E., Sun, D., Russell, C., & Murray, C. (2001). Functionally graded electrical/thermal ceramic systems. Journal of the European Ceramic Society, 21(10-11), 2025-2029.

Noda, N. (1997). Thermal stresses intensity factor for functionally gradient plate with an edge crack. J. Therm. Stresses, 20, 373-387.

Nemat-Alla, M. (2003). Reduction of thermal stresses by developing two-dimensional functionally graded materials. International Journal of Solids and Structures, 40(26), 7339-7356.

Tomota, Y., Kuroki, K., Mori, T., & Tamura T. (1976). Tensile deformation of two–ductile–phase alloys: flow curves of $\alpha \rightarrow \gamma$ Fe–Cr–Ni alloys. Mater. Sci. Eng., 24, 85-94.

K. Wakashima, K., & Tsukamoto, H. (1991). Mean-field micromechanics model and its application to the analysis of thermomechanical behavior of composite materials. Mater. Sci. Eng. A, 146, 291-316.

Levin, V.M. (1967). On the coefficients of thermal expansion of heterogeneous material. Mech. Solids., 2, 88-94.

Mori, T., & Tanaka, K. (1973). Average stress in matrix and average elastic energy of materials with misfittings inclusions. Acta Metallurgica, 21(5), 517-574.

Materials Information Resource MatWeb [Online]. Available: http://www.matweb.com, 2016.

MATLAB. Mathematical software, version 2009a, TheMathWorks, 2009.